# CDKL5 deficiency results in atypical subregion-specific expression of perineuronal nets in the mouse primary visual cortex

Brett Emery*, Matthew Everett*, Billy Y.B. Lau, Keerthi Krishnan

Department of Biochemistry & Molecular and Cellular Biology, University of Tennessee at Knoxville, TN 37996

*Authors contributed equally

Corresponding author: Dr. Keerthi Krishnan, krishnan@utk.edu

ORCiD #:

KK: 0000-0002-0858-4624

BYBL: 0000-0002-2380-5341

**Author Contributions:**

KK supervised the project, designed experiments and analyzed data. BE and ME perfused animals, performed sectioning, immunostained, mapped sections, and manually counted PNNs. BE imaged sections. ME and BYBL performed data analysis and data visualizations. BYBL trained BE and ME in technical aspects of the project. BE, ME, BYBL and KK wrote and edited the manuscript.

**Abstract:**

Cortical perineuronal nets are specialized extracellular matrix structures that form on parvalbumin+ GABAergic neurons, and mark the closure of visual critical period plasticity. More recently, cortical perineuronal nets (PNNs) are used to characterize deficits in critical period plasticity in mouse models for neurodevelopmental disorders such as Rett syndrome, CDKL5 deficiency disorder and Fragile X syndrome. Within the mouse primary visual cortex, studies typically focus on the expression and function of PNNs within the binocular zone, though PNNs are expressed in other subregions of the primary visual cortex. Here, we performed a systematic characterization of wisteria floribunda agglutinin staining, a well-characterized marker for cortical PNNs, in the entire primary visual cortex of wild-type and CDKL5-null male mice. We report a decrease in overall PNN expression in the monocular zone, an increase in high-intensity PNN expression in the binocular zone, and no differences in PNN expression in rostral V1 of CDKL5-null male visual cortex. Additionally, PNN expression was similar across both hemispheres, showing a lack of hemisphere laterality in the early visual cortex. Together, these results suggest that at the closure of the visual critical period plasticity, subregion-specific variations in PNN expression may lead to functional differences in synaptic plasticity in CDKL5-null cortex and lay the groundwork for further studies to probe the roles for PNNs beyond the binocular zone.

## Introduction:

Cortical circuits are shaped by experience during sensitive time windows of early postnatal life. In the developing binocular zone of the visual cortex, these critical periods are crucial for experience-dependent formation of synaptic connectivity, and wiring of neuronal pathways that underlie visual function. The postnatal maturation of cortical interneurons, specifically parvalbumin+ (PV) GABAergic neurons, is critical for controlling the timing of critical period plasticity and visual function (Hensch, 2005; Hensch et al., 1998; Huang et al., 1999; Wang et al., 2010). This postnatal experience-dependent maturation of PV neurons is concomitant with the expression of specialized extracellular matrix structures called perineuronal nets (PNNs) on PV neurons (Begum and Sng, 2017; Gundelfinger et al., 2010; Hartig et al., 1992; Hou et al., 2017; Kosaka and Heizmann, 1989; Krishnan et al., 2015; Nakagawa et al., 1986; Orlando et al., 2012; Sigal et al., 2019; Ueno et al., 2018; Ye and Miao, 2013). PNNs are mainly composed of lecticans, chondroitin sulfate proteoglycans, hyaluronan glycosaminoglycan chains, link proteins and tenascin-R (Bignami et al., 1992; Carulli et al., 2007; Kwok et al., 2010; Miyata and Kitagawa, 2017). Mature PNNs are thought to restrict plasticity, as their removal in adult visual cortex restores ocular dominance plasticity (Beurdeley et al., 2012; Hou et al., 2017; Pizzorusso et al., 2002, 2006). Disruptions to the timing of critical period plasticity via PV neurons, or alterations in GABA transmission and connectivity change PNN expression, affect cortical plasticity and are associated with neurodevelopmental disorders such as Rett syndrome, CDKL5 deficiency disorder and Fragile X syndrome (Carstens et al., 2021; Krishnan et al., 2015; Krishnan et al., 2017; Lau et al., 2020a; Lau et al., 2020b; Patrizi et al., 2020; Pizzo et al., 2016; Reinhard et al., 2019; Wen et al., 2018).

Given the importance of visual critical period plasticity as a paradigm to study experience-dependent processes, and the steady use of Wisteria floribunda agglutinin staining to mark cortical PNNs, here we systematically characterize the expression of this marker in the whole visual cortex (wV1), including the monocular zone (V1M), in the developing mouse visual cortex. This is particularly significant as most of the studies thus far have only focused on the binocular zone (V1B) of the visual cortex. The formation, maintenance and function of PNNs in synaptic plasticity in the wV1 is unclear. We utilized this whole visual cortex dataset and found subregion-, rostra-caudal axis-specific changes in PNN expression in CDKL5-null mouse model (null), compared to age-matched C57BL/6 wild-type controls (WT). Additionally, in both WT and null brains, PNN expression was similar across both hemispheres, showing a lack of hemisphere laterality in the early postnatal visual cortex. These results are in contrast to our previous work showing hemisphere laterality in PNN expression in the adult primary somatosensory cortex (Lau et al., 2020b), suggesting regional- and age-specific changes in PNN expression. Together, these results set the stage for studying the role of PNNs in diverse cortical areas over different ages.

## Materials and Methods:

### Animals

Young male mice (P15, P30, n=5 per genotype, per age used in this study) were maintained on a 12-hour light-dark cycle. Lights turned on at 07:00 AM and the mice received food ad libitum. Genotypes used were CDKL5 hemizygous (B6.129 (FVB) - Cdkl5$^{tm1.1Joez}$/J) (null) and wild type (C57BL/6J) (Wang et al., 2012). All breeders

were obtained from Jax Laboratory. Procedures were conducted in accordance with the National Institutes of Health's Guide for the Care and Use of Laboratory Animals. Protocols were approved by the University of Tennessee in Knoxville's Institutional Animal Care and Use Committee.

**Immunohistochemistry**

On P15 and P30, male null and wild type mice were perfused with 1X phosphate buffer solution (PBS) followed by 4% paraformaldehyde dissolved in PBS. Brains were extracted and post- fixed overnight at 4°C. Prior to sectioning, brains were treated with 30% sucrose in PBS overnight at room temperature. A cut made on the left ventral-medial brain hemisphere to distinguish left-right hemisphere during subsequent tissue processing and analysis. Coronal brain sections at 70µm were collected using a freezing microtome. Immunohistochemistry was performed as previously described (Krishnan et al., 2015). Briefly, free-floating brain sections were blocked in 10% normal goat serum (NGS) and 0.5% Triton-X in PBS for 3 hours. Then, sections were incubated overnight with biotin conjugated Lectin from Wisteria Floribunda (L1516, Sigma-Aldrich) (1:500) in a 5% NGS and 0.25% Triton-X in PBS. Some P15 brain sections were also co-labeled with BCL11B/CTIP2 (PA5-83952, ThermoFisher Scientific) (1:1,000). The next day, sections were incubated for four hours with appropriate secondary antibody (1:1000) in a 5% NGS and 0.25% Triton-X in PBS. In the final step, sections were stained with the marker DAPI (1:1000) for five minutes, and mounted on slides in Fluoromount-G.

**Image Acquisition and Analysis**

For PNN analysis, 10X single-plane PNN images of the entire visual cortex from each brain section were acquired on a motorized stage epifluorescent microscope (Keyence BZ-X710; Keyence Corp.) and stitched using Keyence BZ-X Analyzer. Imaging settings were established based on null (Pizzo et al., 2016) having the most PNN expression compared to the wild type, and standardized across cohorts. After image acquisition, analysis was performed in ImageJ. Rostal V1 (V1), binocular zone (V1B) and monocular zone (V1M) of each image were identified and outlined by overlaying maps from the Paxinos and Franklin's mouse brain atlas (Paxinos and Franklin, 2013). We counted PNNs as previously described (Lau et al., 2020b). Briefly, to count high-intensity mature PNNs, the "contrast" setting from ImageJ was set to the far right to remove weaker signals. The remaining signals were manually quantified as a "mature" PNN if it retained 80% of its original shape (before contrast adjustment) and had proximal processes before contrast adjustment. All PNNs were manually quantified from the 'original' image (no contrast nor brightness adjustment), which included high-intensity PNNs as well. These PNNs are complete in shape with 100% complete borders and proximal processes. All statistical analysis and graphs were generated using GraphPad Prism.

**Results:**

We performed a systematic characterization of PNN expression across the subregions of the visual cortex by collecting all coronal brain sections covering the entire visual cortex (wV1), rather than the standard approach of analyzing representative sample sections (Fig. 1A). We analyzed 10–15 coronal brain sections (at 70 µm each, in both left and right hemispheres) per brain. The wV1 subregions are composed of rostral V1 (V1), monocular zon (V1M) and binocular zone (V1B). They are found at Bregma coordinates -2.15 mm (rostral) to -4.35 mm

(caudal), which encompass ~2.2 mm of the mouse brain (Figure 1B). PNN expression, as assessed by wisteria floribunda agglutinin (WFA) staining, is weak and immature in male wild type mice (WT) early visual cortex development, around P15 (Figure 1C, 1C'). These PNNs surround soma and proximal dendrites of parvalbumin+ GABAergic neurons, and are found predominantly in layer IV, with minimal expression in layer V (Figure 1E). Early identification of deeper cortical layers was performed with co-immunostaining for CTIP2, which labels pyramidal neurons in those layers. By P30, more mature and higher intensity PNNs (Figure 1D, 1D') appear in both V1M and V1B.

As there were too few clear PNN structures at P15 in the different subregions, we focused our further analysis around P30, towards the end of mouse critical period. Qualitatively, in WT, V1M and V1B PNNs were more distinct than rostral V1 (Figure 2A, B), which suggest "immaturity" of PNNs at this time point (Krishnan et al., 2015). By manual quantification of all PNNs (immature and mature PNNs, see Methods for detail) in the visual cortical subregions, we found that V1B had a significantly higher density, in comparison to V1 and V1M (Figure 2C). However, high-intensity PNN (mature PNNs only) density did not differ between the subregions (Figure 2D). The percentage of high-intensity PNNs to all PNNs did not vary significantly between subregions (Figure 2E), suggesting that though there are more PNNs in V1B, a higher proportion of them are not high-intensity or fully mature PNNs. Together, these results suggest expression and maturation of PNNs is subregion-dependent in the mouse visual cortex during the end of critical period.

Next, we determined if the male mouse model for CDKL5 disorder, which was previously shown to have aberrant PNN expression (Pizzo et al, 2016), also displayed subregion-specific changes. Qualitatively, compared to the WT, expression of PNNs in null appeared to be fewer in V1M and with brighter intensity in V1B (Figure 3A, B). Quantitatively, we found that in null, all PNN density was significantly decreased in V1M, with no significant changes in high-intensity PNNs, compared to WT (Figure 3D). In V1B, high-intensity PNN density was significantly higher in null than WT, with no significant differences in all PNN density (Figure 3E). However, we did not observe significant differences in PNN density between WT and null in rostral V1 (Figure 3C). Together, these results suggest that subtle yet significant subregion-specific differences exist in PNN density within the CDKL5-null mouse visual cortex.

Previously, we reported lateral-medial changes in high-intensity PNN density in the primary somatosensory cortex of ~12 week old adult female mice (Lau et al., 2020b). To determine if such anatomical axes differences existed in ~4 week old (P30) male wV1, we plotted individual PNN density per section in the rostral-caudal axis. In contrast to the adult primary somatosensory cortical PNN density distribution, we did not observe significant differences in all or high-intensity PNN density within genotypes along the rostral-caudal axis (Figure 4). Comparing null to WT, we did observe significant decreases in all PNN density in the more caudal areas of null V1M (Figure 4B) and increases in high-intensity PNN density in the rostral areas of null V1B (Figure 4F). We did not observe significant differences in all or high-intensity PNN density between WT and null rostral V1 (V1) along the rostral-caudal axis (Figure 4A, D). Together, these results point to specific disruptions in a subregion- and axis-specific manner in the null visual cortex.

Previously, we reported lateralized, subregion-specific expression of high-intensity PNNs in the 12 weeks old primary somatosensory cortex (Lau et al., 2020b). Thus, we investigated if lateralized PNN expression can be observed in early postnatal development in the wV1. Interestingly, we did not observe significant lateralization in either all or high-intensity PNN expression in wV1 subregions (Figure 5). However, we did note individual brains with lateralized high-intensity PNNs in the rostral V1 (Figure 5C). Together, these results suggest that lateralization of PNNs has not been established at this early stage in the visual cortex and is not dysregulated in the male CDKL5-null visual cortex.

**Discussion:**

PNNs are widely expressed in the rodent brain. Particularly, the different sensory cortical regions display dense PNNs surrounding the soma of neurons. Though their relative functions in individual brain regions and cell types may vary (Balmer, 2016; Carstens et al., 2016; Dauth et al., 2016; Devienne et al., 2021; Krishnan et al., 2017; Tewari et al., 2018), overall PNNs regulate the function of inhibitory networks during development and adulthood. As PNNs are predominantly found on PV+ GABAergic neurons in the cortex, they are intimately associated with and contribute to PV+ network function including gamma oscillations, and ultimately behavior. Thus, determining the function of PNNs in different regions and biological contexts requires a thorough characterization of their expression across the whole brain. Towards this bigger goal, we have focused our efforts on the primary visual cortex during the well-accepted critical period time period.

Most of the knowledge of PNN expression and function in the mouse V1 is based on the binocular zone. The known electrophysiological properties and roles of the binocular zone in ocular dominance plasticity, binocular matching and depth perception have allowed for elucidating the importance of PNNs in brain function. Here, we present the first systematic characterization of PNN expression with subregion-, rostrocaudal axis-, and hemisphere/laterality-specificity in the whole primary visual cortex at the peak of critical period (Figure 6). We report that the absolute density of all PNN expression in the wild-type monocular V1 and rostral V1 is substantial. The functional relevance of this expression in these subregions, with a similar timeline of maturation as V1B, is unclear. Typically, neurons of monocular V1 are thought to encode for receptive field properties including orientation and direction selectivity. However, the role of neuronal activity and/or visual experience in initial formation and maturation of these properties is controversial (Chapman and Stryker, 1993; Hagihara et al., 2015; Ko et al., 2013; Miller et al., 1999). Furthermore, the role of inhibitory neurons in the establishment and maintenance of receptive field properties in monocular V1 remains to be determined. Emergence of multi-unit recordings and wide-field imaging techniques with natural scenery stimuli in different species could begin to shed light on the role of V1M and ultimately, on PV interneurons and PNNs. From representative section analysis, approximately 50% of the PV+ neurons in the binocular zone of the primary visual cortex are surrounded by PNNs. Further systematic whole brain study of double-labeled PNN – PV across the subregions would be a useful resource for the community, and is currently beyond the scope of this study. Furthermore, results from the comparative analysis with CDKL5-null V1 suggest that PNN expression is malleable in all subregions of V1, and is impacted by CDKL5. Future directions involve determining the impact of classical critical

period manipulations such as monocular deprivation or dark rearing on PNN expression and function in the CDKL5-null whole visual cortex.

CDKL5 deficiency disorder is a neurodevelopmental disorder characterized by seizures, intellectual disability, motor and social impairment. Patients with CDKL5 deficiency disorder often exhibit cerebral visual impairment (Brock et al., 2021; Kind and Bird, 2021; Mari et al., 2005; Quintiliani et al., 2021). In null and heterozygous rodent models for CDKL5 deficiency disorder, persistent reduction in response amplitude, reduced visual acuity and defective contrast function are observed by measuring visually evoked potentials (Mazziotti et al., 2017). Interestingly, these deficits in visually evoked responses are observed at the peak of visual critical period plasticity (~P28) and in adults (~P60-80), but not before (~P25). These results correlate with increased expression of PNNs in the binocular zone at ~P35 (Pizzo et al., 2016). Together, these results suggest that the timing of critical period plasticity and proper wiring of visual cortical circuits are affected in rodent models for CDKL5 deficiency disorder. Due to the subtle PNN phenotypes detected in null male mice, we could not justify performing similar visual cortical analysis in heterozygous female mice (CDKL5-heterozygotes), due to the inherent mosaicism and lack of reliable antibodies to label CDKL5 protein in individual cells of the heterozygous females (preliminary data from our lab). Our findings are consistent with these results, and add to the idea that excitation/inhibition imbalance in CDKL5-null V1 is likely to contribute to the visual impairments associated with CDKL5 deficient pathology. Further electrophysiological studies are necessary to determine how a decrease in all PNN expression in V1M, an increase in high-intensity PNN expression in V1B, and no differences in PNN expression in rostral V1 (Figures 3, 6) ultimately contribute to the differentially evoked activity, *in vivo* neural activity and/or synchrony in CDKL5-null wV1. These subregional differences are particularly important in the context of the rostrocaudal position, with intermediate-caudal V1M showing fewer all PNNs, while more V1B showing increase high-intensity PNNs (Figure 4, 6). Such positional information points to nuanced and likely compensatory synaptic plasticity mechanisms in the CDKL5-null brain. As PV neuronal activity influences PNN maintenance, it is likely that PV network activity and/or gamma oscillations are disrupted in a subregion-specific manner in the CDKL5-null whole V1 (Bartos et al., 2002; Devienne et al., 2021).

**Acknowledgments:**

We would like to thank the following undergraduate students for their help with PNN counting and other technical contributions: Sarah-Anne Bowyer and Bailey Bohannon. This work was supported through startup funds to KK and research assistantships to BE and ME from the University of Tennessee, Knoxville.

**References:**

Balmer, T.S., 2016. Perineuronal Nets Enhance the Excitability of Fast-Spiking Neurons. eNeuro 3. https://doi.org/10.1523/ENEURO.0112-16.2016

Bartos, M., Vida, I., Frotscher, M., Meyer, A., Monyer, H., Geiger, J.R.P., Jonas, P., 2002. Fast synaptic inhibition promotes synchronized gamma oscillations in hippocampal interneuron networks. Proc. Natl. Acad. Sci. U. S. A. 99, 13222–13227. https://doi.org/10.1073/pnas.192233099

Begum, M.R., Sng, J.C.G., 2017. Molecular mechanisms of experience-dependent maturation in cortical GABAergic inhibition. J Neurochem 142, 649–661. https://doi.org/10.1111/jnc.14103

Beurdeley, M., Spatazza, J., Lee, H.H.C., Sugiyama, S., Bernard, C., Di Nardo, A.A., Hensch, T.K., Prochiantz, A., 2012. Otx2 Binding to Perineuronal Nets Persistently Regulates Plasticity in the Mature Visual Cortex. J. Neurosci. 32, 9429–9437. https://doi.org/10.1523/JNEUROSCI.0394-12.2012

Bignami, A., Asher, R., Perides, G., 1992. Co-localization of hyaluronic acid and chondroitin sulfate proteoglycan in rat cerebral cortex. Brain Res. 579, 173–177.

Brock, D., Fidell, A., Thomas, J., Juarez-Colunga, E., Benke, T.A., Demarest, S., 2021. Cerebral Visual Impairment in CDKL5 Deficiency Disorder Correlates With Developmental Achievement. J. Child Neurol. 36, 974–980. https://doi.org/10.1177/08830738211019284

Carstens, K.E., Lustberg, D.J., Shaughnessy, E.K., McCann, K.E., Alexander, G.M., Dudek, S.M., 2021. Perineuronal net degradation rescues CA2 plasticity in a mouse model of Rett syndrome. J. Clin. Invest. 131. https://doi.org/10.1172/JCI137221

Carstens, K.E., Phillips, M.L., Pozzo-Miller, L., Weinberg, R.J., Dudek, S.M., 2016. Perineuronal Nets Suppress Plasticity of Excitatory Synapses on CA2 Pyramidal Neurons. J. Neurosci. 36, 6312–6320. https://doi.org/10.1523/JNEUROSCI.0245-16.2016

Carulli, D., Rhodes, K.E., Fawcett, J.W., 2007. Upregulation of aggrecan, link protein 1, and hyaluronan synthases during formation of perineuronal nets in the rat cerebellum. J Comp Neurol 501, 83–94. https://doi.org/10.1002/cne.21231

Chapman, B., Stryker, M., 1993. Development of orientation selectivity in ferret visual cortex and effects of deprivation. J. Neurosci. 13, 5251–5262. https://doi.org/10.1523/JNEUROSCI.13-12-05251.1993

Dauth, S., Grevesse, T., Pantazopoulos, H., Campbell, P.H., Maoz, B.M., Berretta, S., Parker, K.K., 2016. Extracellular matrix protein expression is brain region dependent. J. Comp. Neurol. 524, 1309–1336. https://doi.org/10.1002/cne.23965

Devienne, G., Picaud, S., Cohen, I., Piquet, J., Tricoire, L., Testa, D., Di Nardo, A.A., Rossier, J., Cauli, B., Lambolez, B., 2021. Regulation of perineuronal nets in the adult cortex by the activity of the cortical network. J. Neurosci. Off. J. Soc. Neurosci. JN-RM-0434-21. https://doi.org/10.1523/JNEUROSCI.0434-21.2021

Gundelfinger, E.D., Frischknecht, R., Choquet, D., Heine, M., 2010. Converting juvenile into adult plasticity: a role for the brain's extracellular matrix. Eur. J. Neurosci. 31, 2156–2165. https://doi.org/10.1111/j.1460-9568.2010.07253.x

Hagihara, K.M., Murakami, T., Yoshida, T., Tagawa, Y., Ohki, K., 2015. Neuronal activity is not required for the initial formation and maturation of visual selectivity. Nat. Neurosci. 18, 1780–1788. https://doi.org/10.1038/nn.4155

Hartig, W., Brauer, K., Bruckner, G., 1992. Wisteria floribunda agglutinin-labelled nets surround parvalbumin-containing neurons. Neuroreport 3, 869–72.

Hensch, T.K., 2005. Critical period mechanisms in developing visual cortex. Curr Top Dev Biol 69, 215–37. https://doi.org/10.1016/s0070-2153(05)69008-4

Hensch, T.K., Gordon, J.A., Brandon, E.P., McKnight, G.S., Idzerda, R.L., Stryker, M.P., 1998. Comparison of Plasticity In Vivo and In Vitro in the Developing Visual Cortex of Normal and Protein Kinase A RIβ-Deficient Mice. J. Neurosci. 18, 2108–2117. https://doi.org/10.1523/JNEUROSCI.18-06-02108.1998

Hou, X., Yoshioka, N., Tsukano, H., Sakai, A., Miyata, S., Watanabe, Y., Yanagawa, Y., Sakimura, K., Takeuchi, K., Kitagawa, H., Hensch, T.K., Shibuki, K., Igarashi, M., Sugiyama, S., 2017. Chondroitin Sulfate Is Required for Onset and Offset of Critical Period Plasticity in Visual Cortex. Sci. Rep. 7, 12646. https://doi.org/10.1038/s41598-017-04007-x

Huang, Z.J., Kirkwood, A., Pizzorusso, T., Porciatti, V., Morales, B., Bear, M.F., Maffei, L., Tonegawa, S., 1999. BDNF regulates the maturation of inhibition and the critical period of plasticity in mouse visual cortex. Cell 98, 739–755. https://doi.org/10.1016/s0092-8674(00)81509-3

Kind, P.C., Bird, A., 2021. CDKL5 deficiency disorder: a pathophysiology of neural maintenance. J. Clin. Invest. 131, e153606. https://doi.org/10.1172/JCI153606

Ko, H., Cossell, L., Baragli, C., Antolik, J., Clopath, C., Hofer, S.B., Mrsic-Flogel, T.D., 2013. The emergence of functional microcircuits in visual cortex. Nature 496, 96–100. https://doi.org/10.1038/nature12015

Kosaka, T., Heizmann, C.W., 1989. Selective staining of a population of parvalbumin-containing GABAergic neurons in the rat cerebral cortex by lectins with specific affinity for terminal N-acetylgalactosamine. Brain Res. 483, 158–163. https://doi.org/10.1016/0006-8993(89)90048-6

Krishnan, K., Lau, B.Y.B., Ewall, G., Huang, Z.J., Shea, S.D., 2017. MECP2 regulates cortical plasticity underlying a learned behaviour in adult female mice. Nat. Commun. 8, 14077.

Krishnan, K., Wang, B.-S., Lu, J., Wang, L., Maffei, A., Cang, J., Huang, Z.J., 2015. MeCP2 regulates the timing of critical period plasticity that shapes functional connectivity in primary visual cortex. Proc. Natl. Acad. Sci. U. S. A. 112, E4782-4791. https://doi.org/10.1073/pnas.1506499112

Kwok, J.C.F., Carulli, D., Fawcett, J.W., 2010. In vitro modeling of perineuronal nets: hyaluronan synthase and link protein are necessary for their formation and integrity: Hyaluronan synthase and link protein in PNNs. J. Neurochem. no-no. https://doi.org/10.1111/j.1471-4159.2010.06878.x

Lau, Billy Y.B., Krishnan, K., Huang, Z.J., Shea, S.D., 2020. Maternal Experience-Dependent Cortical Plasticity in Mice Is Circuit- and Stimulus-Specific and Requires MECP2. J. Neurosci. 40, 1514–1526. https://doi.org/10.1523/JNEUROSCI.1964-19.2019

Lau, Billy Y. B., Layo, D.E., Emery, B., Everett, M., Kumar, A., Stevenson, P., Reynolds, K.G., Cherosky, A., Bowyer, S.-A.H., Roth, S., Fisher, D.G., McCord, R.P., Krishnan, K., 2020. Lateralized Expression of Cortical Perineuronal Nets during Maternal Experience is Dependent on MECP2. eneuro 7, ENEURO.0500-19.2020. https://doi.org/10.1523/ENEURO.0500-19.2020

Mari, F., Azimonti, S., Bertani, I., Bolognese, F., Colombo, E., Caselli, R., Scala, E., Longo, I., Grosso, S., Pescucci, C., Ariani, F., Hayek, G., Balestri, P., Bergo, A., Badaracco, G., Zappella, M., Broccoli, V., Renieri, A., Kilstrup-Nielsen, C., Landsberger, N., 2005. CDKL5 belongs to the same molecular pathway of MeCP2 and it is responsible for the

early-onset seizure variant of Rett syndrome. Hum. Mol. Genet. 14, 1935–1946. https://doi.org/10.1093/hmg/ddi198

Mazziotti, R., Lupori, L., Sagona, G., Gennaro, M., Della Sala, G., Putignano, E., Pizzorusso, T., 2017. Searching for biomarkers of CDKL5 disorder: early-onset visual impairment in CDKL5 mutant mice. Hum. Mol. Genet. 26, 2290–2298. https://doi.org/10.1093/hmg/ddx119

Miller, K.D., Erwin, E., Kayser, A., 1999. Is the development of orientation selectivity instructed by activity? J. Neurobiol. 41, 44–57. https://doi.org/10.1002/(SICI)1097-4695(199910)41:1<44::AID-NEU7>3.0.CO;2-V

Miyata, S., Kitagawa, H., 2017. Formation and remodeling of the brain extracellular matrix in neural plasticity: Roles of chondroitin sulfate and hyaluronan. Biochim Biophys Acta 1861, 2420–2434. https://doi.org/10.1016/j.bbagen.2017.06.010

Nakagawa, F., Schulte, B.A., Wu, J.Y., Spicer, S.S., 1986. GABAergic neurons of rodent brain correspond partially with those staining for glycoconjugate with terminal N-acetylgalactosamine. J. Neurocytol. 15, 389–396.

Orlando, C., Ster, J., Gerber, U., Fawcett, J.W., Raineteau, O., 2012. Perisynaptic Chondroitin Sulfate Proteoglycans Restrict Structural Plasticity in an Integrin-Dependent Manner. J. Neurosci. 32, 18009–18017. https://doi.org/10.1523/JNEUROSCI.2406-12.2012

Patrizi, A., Awad, P.N., Chattopadhyaya, B., Li, C., Di Cristo, G., Fagiolini, M., 2020. Accelerated Hyper-Maturation of Parvalbumin Circuits in the Absence of MeCP2. Cereb. Cortex N. Y. N 1991 30, 256–268. https://doi.org/10.1093/cercor/bhz085

Pizzo, R., Gurgone, A., Castroflorio, E., Amendola, E., Gross, C., Sassoè-Pognetto, M., Giustetto, M., 2016. Lack of Cdkl5 Disrupts the Organization of Excitatory and Inhibitory Synapses and Parvalbumin Interneurons in the Primary Visual Cortex. Front. Cell. Neurosci. 10, 261. https://doi.org/10.3389/fncel.2016.00261

Pizzorusso, T., Medini, P., Berardi, N., Chierzi, S., Fawcett, J.W., Maffei, L., 2002. Reactivation of ocular dominance plasticity in the adult visual cortex. Science 298, 1248–1251. https://doi.org/10.1126/science.1072699

Pizzorusso, T., Medini, P., Landi, S., Baldini, S., Berardi, N., Maffei, L., 2006. Structural and functional recovery from early monocular deprivation in adult rats. Proc. Natl. Acad. Sci. 103, 8517–8522. https://doi.org/10.1073/pnas.0602657103

Quintiliani, M., Ricci, D., Petrianni, M., Leone, S., Orazi, L., Amore, F., Gambardella, M.L., Contaldo, I., Veredice, C., Perulli, M., Musto, E., Mercuri, E.M., Battaglia, D.I., 2021. Cortical Visual Impairment in CDKL5 Deficiency Disorder. Front. Neurol. 12, 805745. https://doi.org/10.3389/fneur.2021.805745

Reinhard, S.M., Rais, M., Afroz, S., Hanania, Y., Pendi, K., Espinoza, K., Rosenthal, R., Binder, D.K., Ethell, I.M., Razak, K.A., 2019. Reduced perineuronal net expression in Fmr1 KO mice auditory cortex and amygdala is linked to impaired fear-associated memory. Neurobiol. Learn. Mem. 164, 107042. https://doi.org/10.1016/j.nlm.2019.107042

Sigal, Y.M., Bae, H., Bogart, L.J., Hensch, T.K., Zhuang, X., 2019. Structural maturation of cortical perineuronal nets and their perforating synapses revealed by superresolution imaging. Proc. Natl. Acad. Sci. U. S. A. 116, 7071–7076. https://doi.org/10.1073/pnas.1817222116

Tewari, B.P., Chaunsali, L., Campbell, S.L., Patel, D.C., Goode, A.E., Sontheimer, H., 2018. Perineuronal nets decrease membrane capacitance of peritumoral fast spiking interneurons in a model of epilepsy. Nat. Commun. 9, 4724. https://doi.org/10.1038/s41467-018-07113-0

Ueno, H., Takao, K., Suemitsu, S., Murakami, S., Kitamura, N., Wani, K., Okamoto, M., Aoki, S., Ishihara, T., 2018. Age-dependent and region-specific alteration of parvalbumin neurons and perineuronal nets in the mouse cerebral cortex. Neurochem. Int. 112, 59–70. https://doi.org/10.1016/j.neuint.2017.11.001

Wang, B.-S., Sarnaik, R., Cang, J., 2010. Critical Period Plasticity Matches Binocular Orientation Preference in the Visual Cortex. Neuron 65, 246–256. https://doi.org/10.1016/j.neuron.2010.01.002

Wang, I.-T.J., Allen, M., Goffin, D., Zhu, X., Fairless, A.H., Brodkin, E.S., Siegel, S.J., Marsh, E.D., Blendy, J.A., Zhou, Z., 2012. Loss of CDKL5 disrupts kinome profile and event-related potentials leading to autistic-like phenotypes in mice. Proc. Natl. Acad. Sci. U. S. A. 109, 21516–21521. https://doi.org/10.1073/pnas.1216988110

Wen, T.H., Afroz, S., Reinhard, S.M., Palacios, A.R., Tapia, K., Binder, D.K., Razak, K.A., Ethell, I.M., 2018. Genetic Reduction of Matrix Metalloproteinase-9 Promotes Formation of Perineuronal Nets Around Parvalbumin-Expressing Interneurons and Normalizes Auditory Cortex Responses in Developing Fmr1 Knock-Out Mice. Cereb. Cortex 28, 3951–3964. https://doi.org/10.1093/cercor/bhx258

Ye, Q., Miao, Q., 2013. Experience-dependent development of perineuronal nets and chondroitin sulfate proteoglycan receptors in mouse visual cortex. Matrix Biol. 32, 352–363. https://doi.org/10.1016/j.matbio.2013.04.001

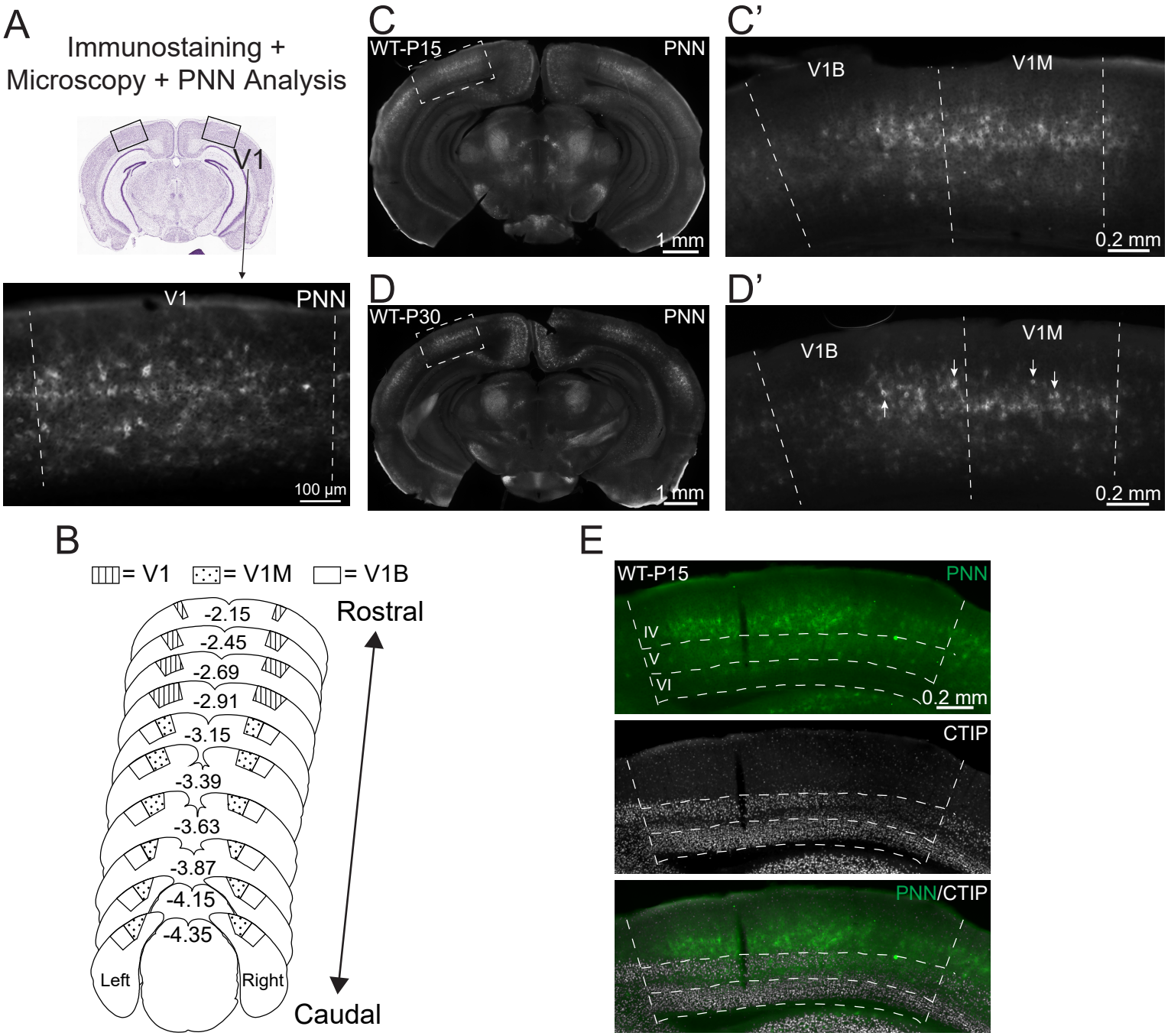
A
Immunostaining +
Microscopy + PNN Analysis
V1
V1
PNN
100 µm
C
WT-P15
PNN
1 mm
C'
V1B
V1M
0.2 mm
D
WT-P30
PNN
1 mm
D'
V1B
V1M
0.2 mm
B
= V1
= V1M
= V1B
Rostral
-2.15
-2.45
-2.69
-2.91
-3.15
-3.39
-3.63
-3.87
-4.15
-4.35
Left
Right
Caudal
E
WT-P15
PNN
IV
V
VI
0.2 mm
CTIP
PNN/CTIP

Figure 1

**Figure 1: Expression of PNNs in subregions of the whole visual cortex (wV1) during WT critical period. (A)** Schema representing mouse brain section (top), and immunostaining with WFA to identify PNNs (bottom). **(B)** Schema of coronal mouse brain sections, depicting rostral to caudal subregions of wV1 analyzed for this study. **(C-D)** Representative epifluorescent images of PNN expression at P15 (C) and P30 (D) of WT. Boxed regions highlight the binocular (V1B) and monocular (V1M) zones and are magnified in C' (P15) and D' (P30). High-intensity PNNs, used for quantification in this study, are marked with arrows. **(E)** Representative epifluorescent images of P15 WT showing PNN expression (green) in layer IV, with minimal co-labeling with layers V and VI cells, as identified by CTIP2 expression (grey).

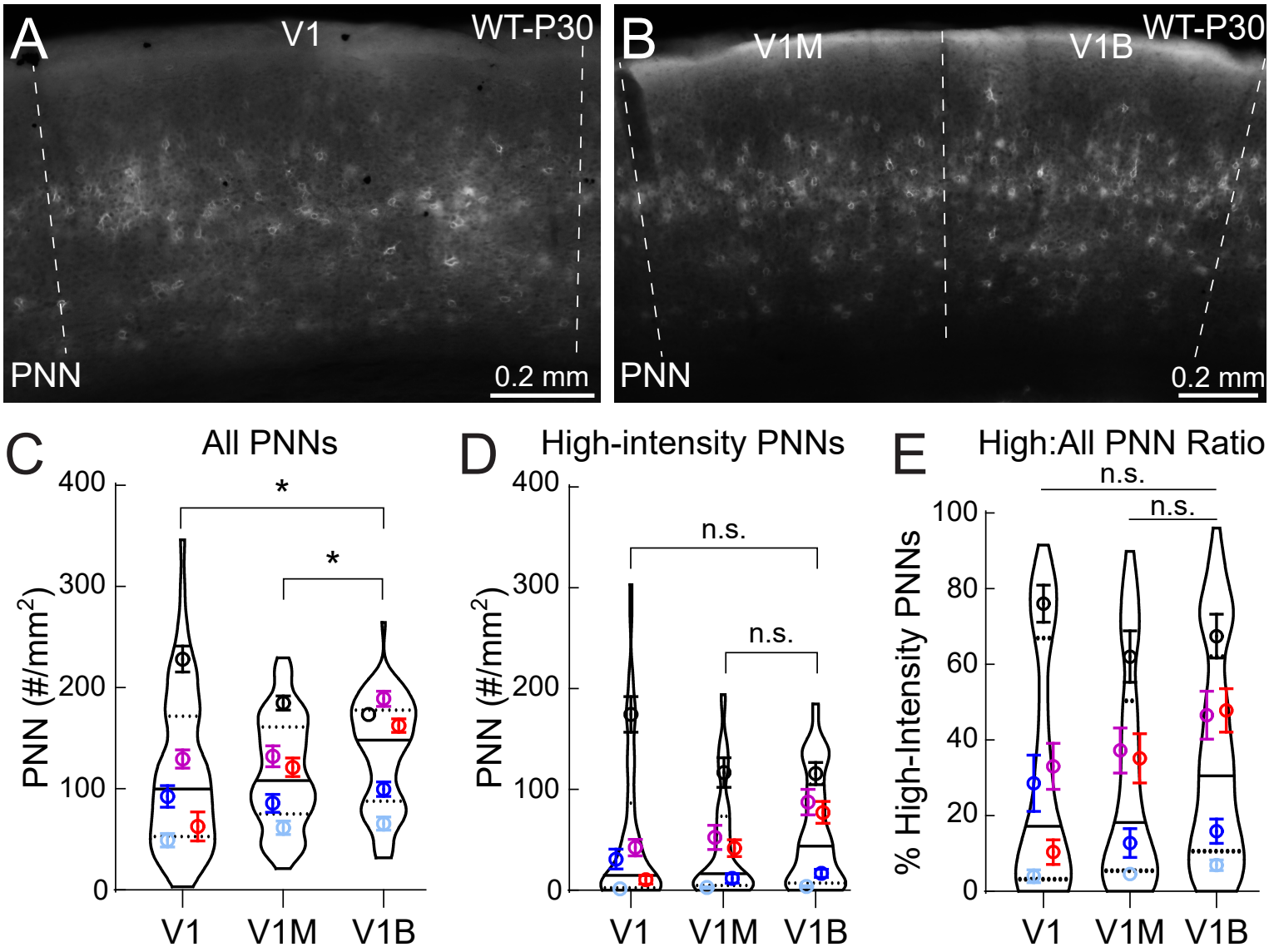
A
V1
WT-P30
PNN
0.2 mm
B
V1M
V1B
WT-P30
PNN
0.2 mm
C
All PNNs
PNN (#/mm2)
400
300
200
100
0
*
*
V1
V1M
V1B
D
High-intensity PNNs
PNN (#/mm2)
400
300
200
100
0
n.s.
n.s.
V1
V1M
V1B
E
High:All PNN Ratio
% High-Intensity PNNs
100
80
60
40
20
0
n.s.
n.s.
V1
V1M
V1B

Figure 2

**Figure 2: Binocular zone of V1 exhibits higher PNN density than other subregions at P30 WT. (A-B)** Representative epifluorescent images of PNN expression in rostral V1 (V1, A), monocular (V1M) and binocular (V1B) zones (B). **(C)** V1B exhibited significantly higher all-PNN density, compared to V1M and V1. **(D)** No significant differences were observed in high-intensity PNNs between all 3 subregions. **(E)** Statistical analysis of high-intensity to All PNN ratio revealed no significant differences between subregions. For C-E, V1 (64 images), V1M (76 images) and V1B (76 images). *Kruskal-Wallis followed by Dunn's test*, $*p < 0.05$, *n.s. = no significance*. Super plots show median (solid line), 25th and 75th quartiles (dash lines) with maximum and minimum, width of violins represents frequency of data points in each region. Each circle + lines represent mean ± s.e.m. for each color-coded cohort.

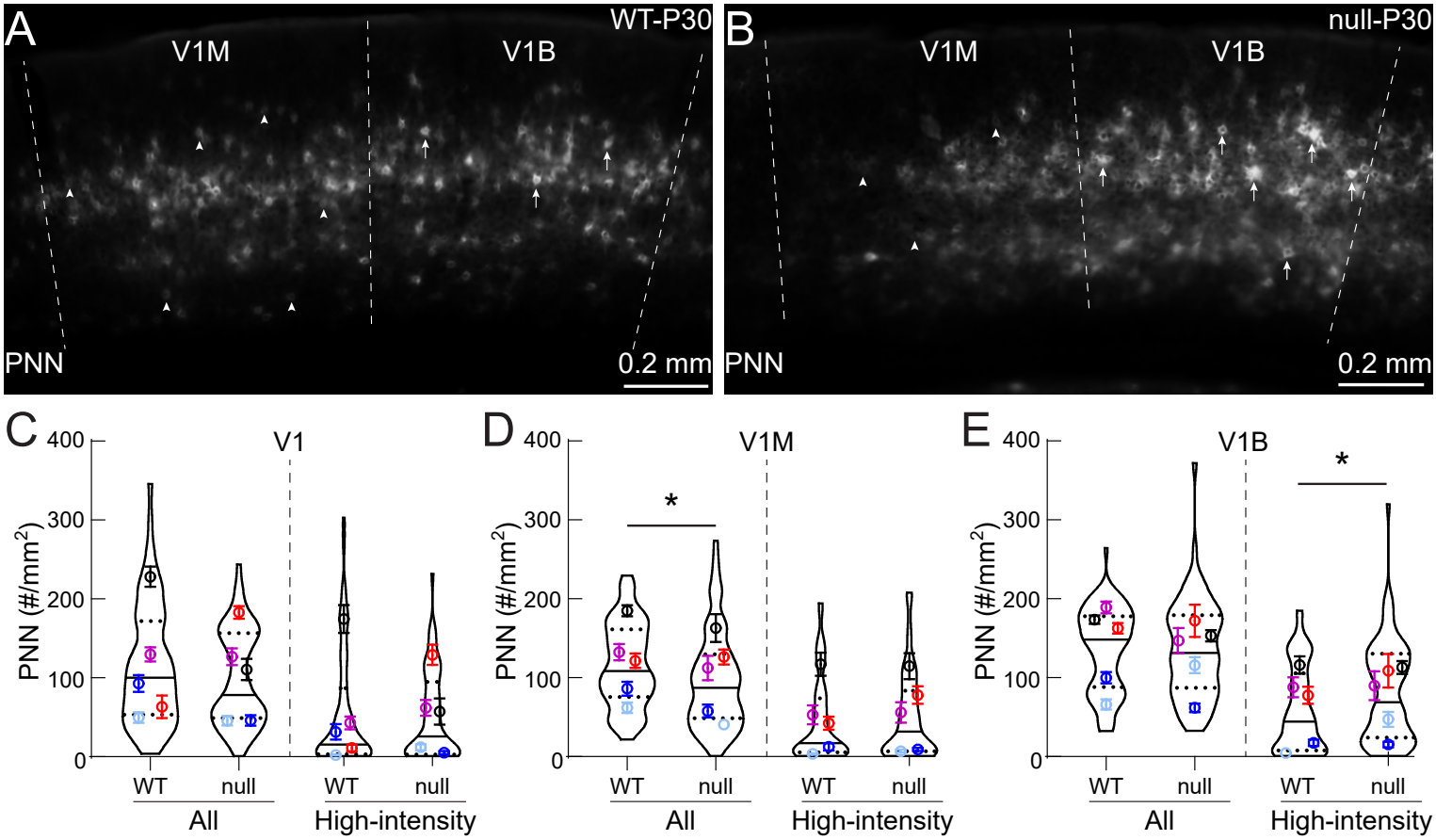
A
WT-P30
V1M
V1B
PNN
0.2 mm
B
null-P30
V1M
V1B
PNN
0.2 mm
C
V1
PNN (#/mm2)
400
300
200
100
0
WT
null
WT
null
All
High-intensity
D
V1M
*
PNN (#/mm2)
WT
null
WT
null
All
High-intensity
E
V1B
*
PNN (#/mm2)
WT
null
WT
null
All
High-intensity

# Figure 3

**Figure 3: Subregion-specific changes in PNN expression in male CKLD5-null mice. (A-B)** Representative epifluorescent images of PNN expression at P30 in V1M and V1B of WT (A) and CDKL5-null (null) (B) show fewer PNNs in V1M, and higher intensity in V1B. Arrowheads and arrows indicate lower intensity and high-intensity PNNs, respectively. **(C)** In rostral V1 (V1), PNN densities were not significantly different between WT and null (WT: n = 64 images; null: n = 62 images; *Mann-Whitney test*, $p = 0.059$). **(D)** However, in V1M, null showed significantly decreased density of all PNNs, with no change in high-intensity PNNs. **(E)** In V1B, null did not show significant change in all PNN density, but expressed significantly more high-intensity PNNs. For D and E, WT: n = 76 images; null: n = 72 images; *Mann-Whitney test,* $*p < 0.05$. For C-E, super plots: violin plots show median (solid line), 25th and 75th quartiles (dash lines) with maximum and minimum, width of violins represents frequency of data points in each region. Circles + lines represent mean ± s.e.m. for each color-coded cohort.

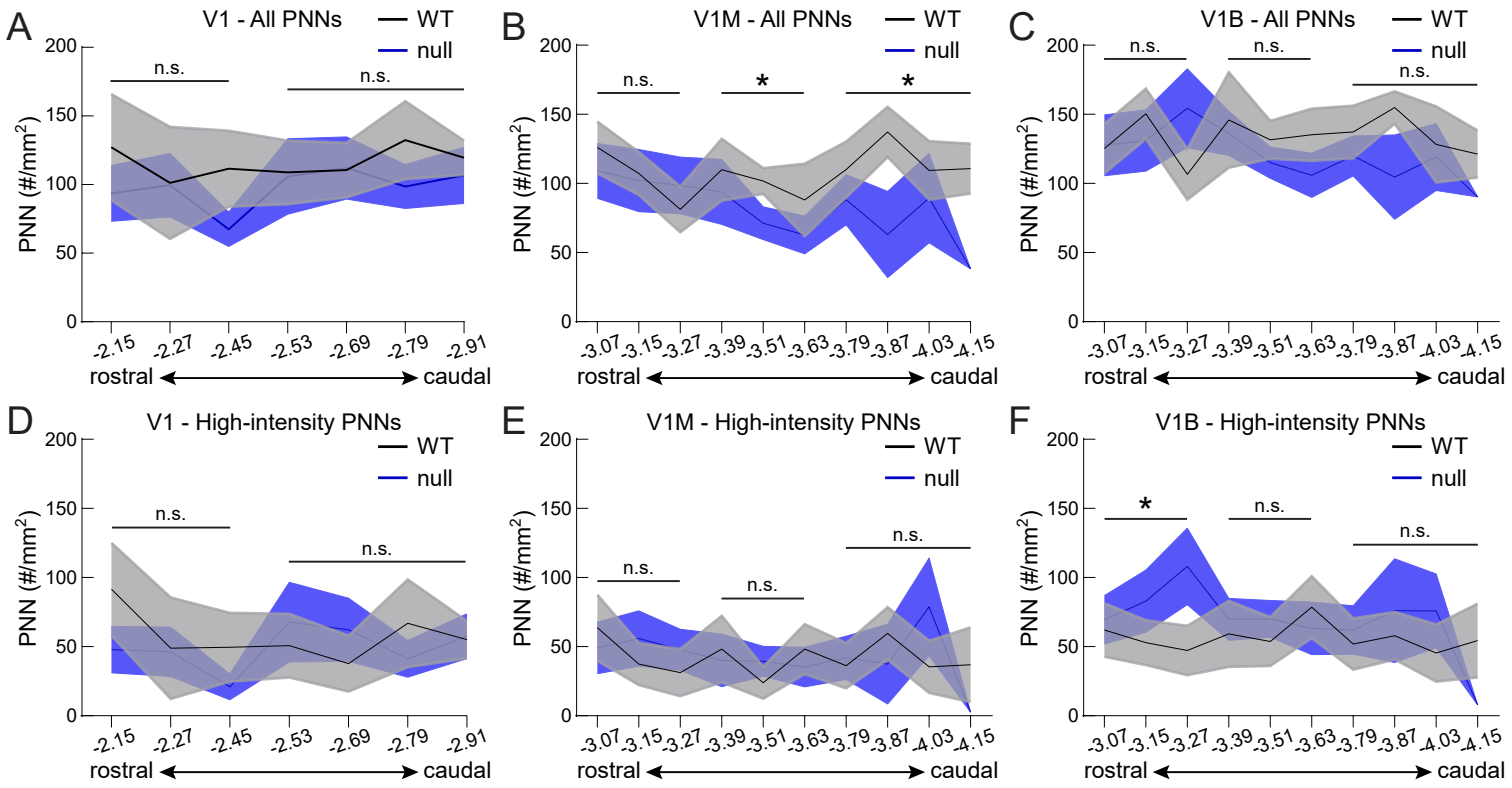
A
V1 - All PNNs
WT
null
n.s.
n.s.
PNN (#/mm²)
200
150
100
50
0
-2.15
-2.27
-2.45
-2.53
-2.69
-2.79
-2.91
rostral
caudal
B
V1M - All PNNs
WT
null
n.s.
*
*
-3.07
-3.15
-3.27
-3.39
-3.51
-3.63
-3.79
-3.87
-4.03
-4.15
C
V1B - All PNNs
n.s.
n.s.
n.s.
D
V1 - High-intensity PNNs
n.s.
n.s.
E
V1M - High-intensity PNNs
n.s.
n.s.
n.s.
F
V1B - High-intensity PNNs
*
n.s.
n.s.

# Figure 4

**Figure 4: P30 CDKL5-null males exhibit altered PNN expression in specific subregions of visual cortex. (A-F)** Distribution of all PNN density (A-C) and high-intensity PNN density (D-F) in WT (grey) and null (blue) in rostral V1 (A, D), V1M (B, E), and V1B (C, F) across rostral-caudal axis. Null exhibited a significant reduction in all PNN density in more caudal regions of V1M (B) and a significant increase in high-intensity PNN density in rostral V1B (F). N = 1-13 images per Bregma coordinate. Solid lines + shades represent mean ± s.e.m. *Mann-Whitney test* within each subregion between WT and null: *$p < 0.05$, *n.s. = no significance*.

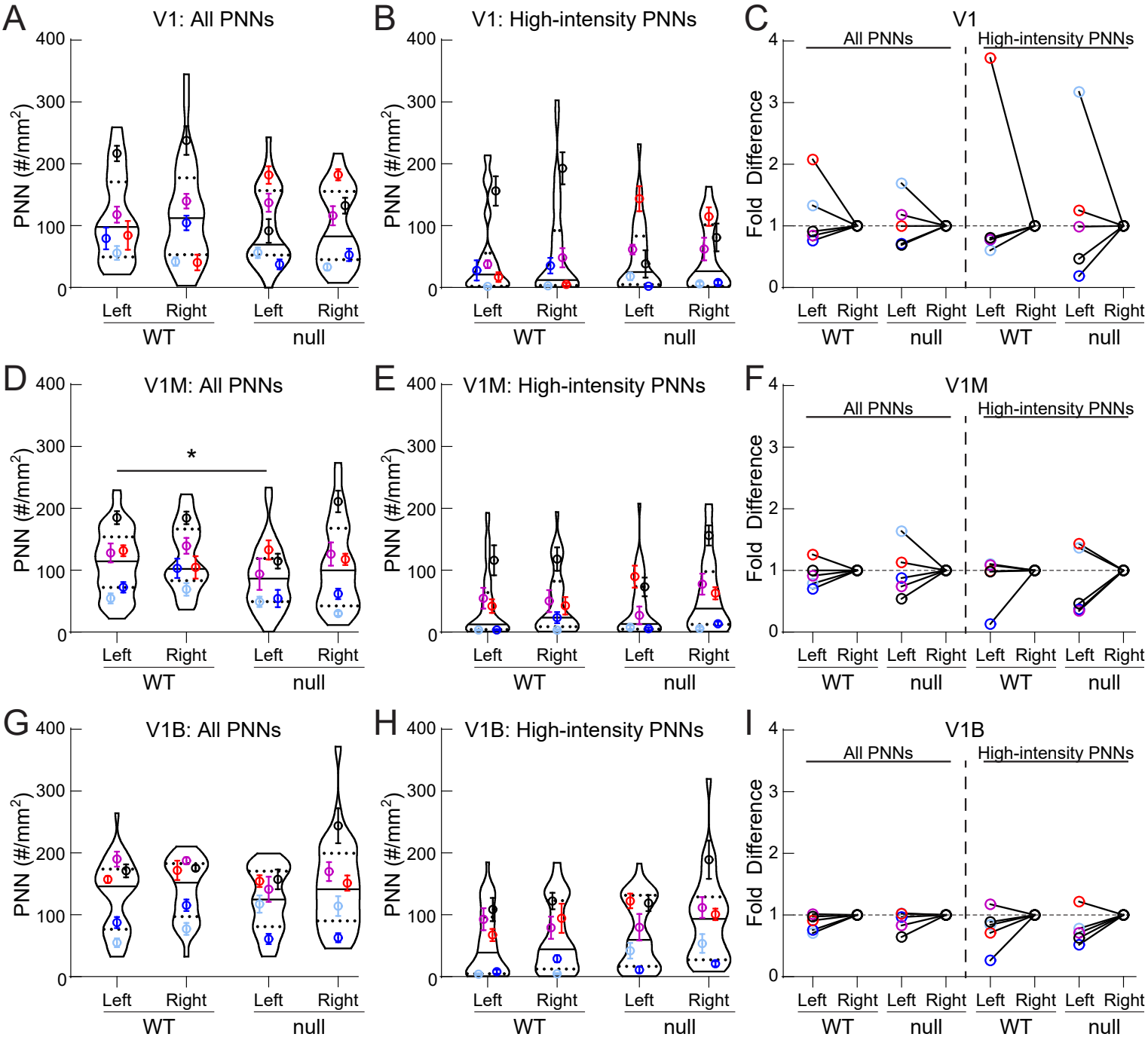
A
V1: All PNNs
B
V1: High-intensity PNNs
C
V1
All PNNs
High-intensity PNNs
D
V1M: All PNNs
E
V1M: High-intensity PNNs
F
V1M
G
V1B: All PNNs
H
V1B: High-intensity PNNs
I
V1B
PNN (#/mm²)
Fold Difference
Left
Right
WT
null
*

# Figure 5

**Figure 5: Individual brains exhibit similar hemispheric PNN density in all V1 subregions.** On average and within genotype, WT and null displayed no asymmetry in all PNN expression **(A, D, G)** or in high-intensity PNNs **(B, E, H)** between hemispheres of rostral V1 (A, B), V1M (D, E) and V1B (G, H). Overall, there were no hemisphere-specific changes between WT and null visual cortex, except for V1M, where null showed a significant reduction in all PNN density in the left hemisphere (D). **(C, F, I)** Individual brains displayed natural variations in asymmetry in both all PNN and high intensity PNN densities in rostral V1 (C), and minimally in V1M (F) and V1B (I). For each brain, PNN density from the left hemisphere was normalized to its right hemisphere. (A-B, D-E, G-H) Super plots: violin plots showing median (solid line), 25th and 75th quartiles (dash lines) with maximum and minimum, width of violins represents frequency of data points in each region. Each circle + lines represent mean ± s.e.m. for each color-coded cohort. N = 31-42 images. *Kruskal-Wallis followed by Dunn's test*, $*p < 0.05$.

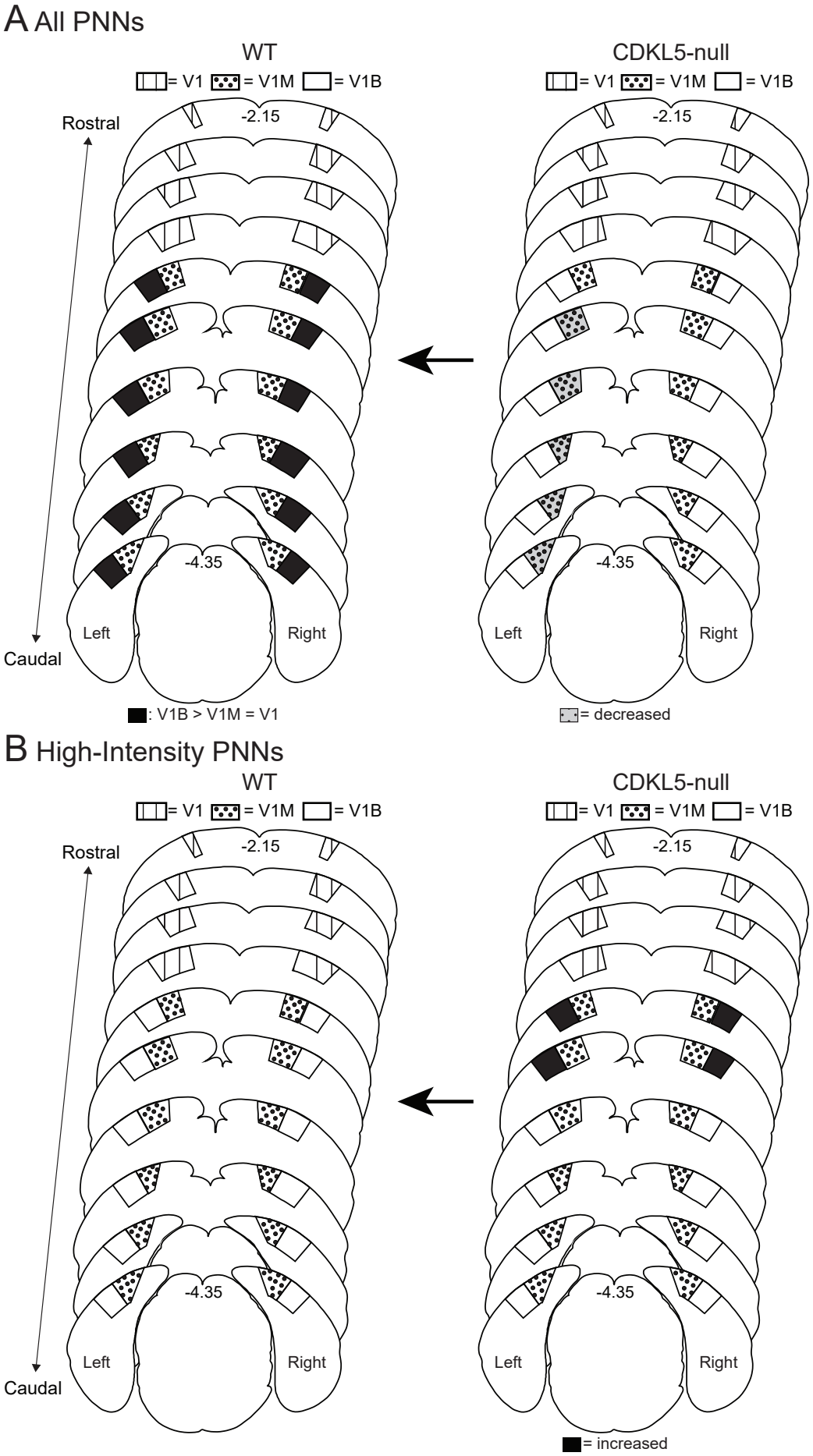
A All PNNs
WT
CDKL5-null
= V1
= V1M
= V1B
Rostral
Caudal
-2.15
-4.35
Left
Right
: V1B > V1M = V1
= decreased
B High-Intensity PNNs
WT
CDKL5-null
= V1
= V1M
= V1B
Rostral
Caudal
-2.15
-4.35
Left
Right
= increased

Figure 6

**Figure 6: Summary diagram - Perineuronal net populations in the primary visual cortex vary by monocular, binocular and rostral subregions.** Overall, WT and CDKL5-null male brains express more overall PNNs in the binocular zone relative to rostral V1 and monocular zone within genotype **(A: left, only WT is shown)**, while expressing similar level of high-intensity PNNs throughout the whole V1 **(B: left, only WT is shown)**. Compared to WT (**arrow in A, B**), CDKL5-null have lesser overall PNN expression in the left hemisphere of the monocular zone **(A: right, grey)**, more high-intensity PNN expression in both hemispheres of the binocular zone **(B: right, black)**, and no difference in rostral V1 (A, B). These results suggest that at the closure of the visual critical period plasticity, subregion-specific variations in PNN expression could lead to functional differences in synaptic plasticity and ultimately, changes in visual function in male CDKL5-null mice. The systematic characterization of PNNs in the rostral-caudal axis lay the groundwork to probe the roles for PNNs beyond the binocular zone of the mouse primary visual cortex.